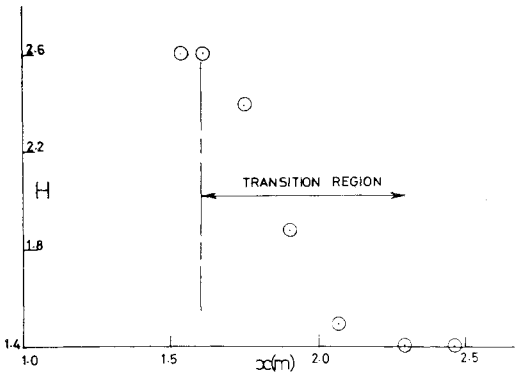

Fig. 4 Distribution of profile shape factor for two-dimensional flat-plate flow (after Schubauer and Klebanoff[8]).

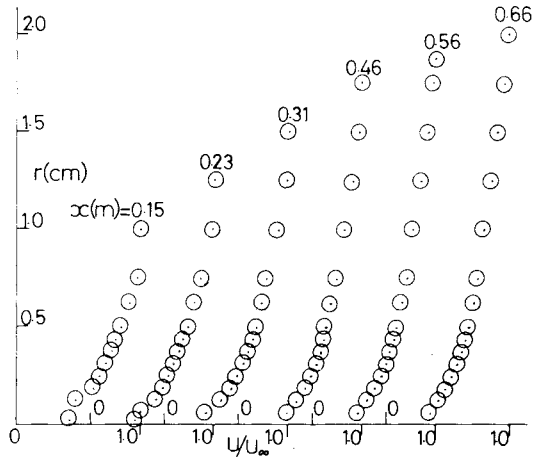

Fig. 5 Development of velocity profiles along the corner bisector with artificial transition.

Artificial Transition

An attempt was made by the present author to examine some aspects of corner flow sensitivity to artificial transition – provoking devices of different mean roughness heights. On the recommendation of Klebanoff and Diehl,[9] who had made a thorough study of tripping devices in two-dimensional flow, sandpaper-type roughness was chosen for the investigation.

With a sandpaper roughness 25.4-mm wide and 0.75-mm high and with its upstream edge 25.4-mm downstream of the corner leading edge, the mean velocity profiles immediately downstream of the transition trip showed, in Fig. 5, some distortion. Fortunately, however, for lack of a sustaining mechanism, the distortion died out fairly quickly in the downstream direction, leaving behind at least some thickening of the boundary layer. Although the tendency toward a "self-preserving" turbulent corner flow was rapid, it was not as rapid as with natural transition. Moreover, the self-preserving form obtained with artificial transition need not be identical with that for natural transition. As a matter of fact, the shape factor H_s [defined by Eq. (1)] of the velocity profile at $x = 1.091$ m with the 0.75-mm transition trip is 1.6, which is about 7% higher than the value 1.5 (Fig. 3), corresponding to the case of natural transition.

References

[1]Mojola, O.O., "Turbulent Boundary Layer Along a Streamwise Corner," Ph.D. thesis, 1972, University of London, London England.

[2]Zamir, M., "Boundary-Layer Flow in a Streamwise Corner," Ph.D. thesis, 1968, University of London, London, England.

[3]Mojola, O.O and Young, A.D., "An Experimental Investigation of the Turbulent Boundary Layer Along a Streamwise Corner," *Proceedings, AGARD Conference on Turbulent Shear Flows*, Sept. 1971, Paper No. 12, London.

[4]Nomura, Y., "Theoretical and Experimental Investigations of the Incompressible Viscous Flow around the Corner," *Memoirs of the Defence Academy of Japan*, Vol. 2, No. 3, 1962.

[5]Zamir, M. and Young, A.D. "Experimental Investigation of the Bounary Layer in a Streamwise Corner," *The Aeronautical Quarterly*, Vol. XXI, Nov. 1970, pp. 313-339.

[6]Gersten, K., "Corner Interference Effects," AGARD Rept. 299, 1959.

[7]Perkins, H.J., "The Turbulent Corner Boundary Layer," Ph.D. thesis, 1970, University of Cambridge, Cambridge, England.

[8]Schubauer, G.B. and Klebanoff, P.S., "Contributions on the Mechanics of Boundary-Layer Transition," NACA TN3489, 1955; also NACA Rept. 1289, 1956.

[9]Klebanoff, P.S. and Diehl, Z.W., "Some Features of Artificially Thickened Fully Developed Turbulent Boundary Layers with Zero Pressure Gradient," NACA Rept. 1110, 1952.

High-Potential Clouds in Jet-Engine Exhausts

J. F. Shaeffer* and T. C. Peng*
McDonnell Douglas Corporation, St. Louis, Mo.

Introduction

EXPERIMENTAL investigations conducted by the Air Force Flight Dynamics Laboratory (AFFDL) have shown that electrostatic probes placed in a jet-engine exhaust to measure ion concentrations produce unusual signal pulses (spikes). In some tests, the occurence of pulses increased by orders of magnitude prior to failure of a gas-path engine component. Initial hopes were that this phenomenon could be utilized to indicate imminent engine failure. However, the mechanism responsible for spike production must be determined, and the relationship to gas-path component failure must be understood. This Note deals with an investigation of potential mechanisms responsible for producing the probe spike signals.

Analyses of AFFDL data and our experiments lead to the conclusion that the observed spikes are a form of negative corona (electrical discharge) known as Trichel pulses. Furthermore, probe data indicate that this negative corona is induced by positively charged, high-potential eddies or clouds which flow past the probe.

The jet-engine related experimental work was conducted by AFFDL and three industrial contractors.[1,2†] The Electrostatic probes used in these studies were 6.3-mm diam, 7.6 to 12.7-cm-long stainless-steel cylinders with well rounded tips. The probes were electrically connected to ground (engine case) through a low-impedance, current-measuring shunt.

A typical single pulse is shown in Fig. 1a. The rise time was comparable to the response time of the instrumentation used (2-4 ns). The decay time was 0.7 μs is this case, but varied between 0.2 and 5 μs. The peak amplitude also varied widely, from 10 mV to several volts, corresponding to peak currents of 100 nA to tens of milliamperes. The total charge (i.e., the time integral of the current) ranged from 0.1 to 10 nC. Pulse polarity was positive, corresponding to positive ions arriving at the probe from the gas or to electrons leaving the probe and

Received July 12, 1976; presented as Paper 76-397 at the AIAA 9th Fluid and Plasma Dynamics Conference, San Diego, Calif., July 14-16, 1976; revision received Nov. 22, 1976

Index categories: Plasma Dynamics and MHD; Combustion in Gases; Atomic, Molecular, and Plasma Properties.

*Scientist, McDonnell Douglas Research Laboratories. Member AIAA.

†References 1 and 2 contain a complete list of citations.

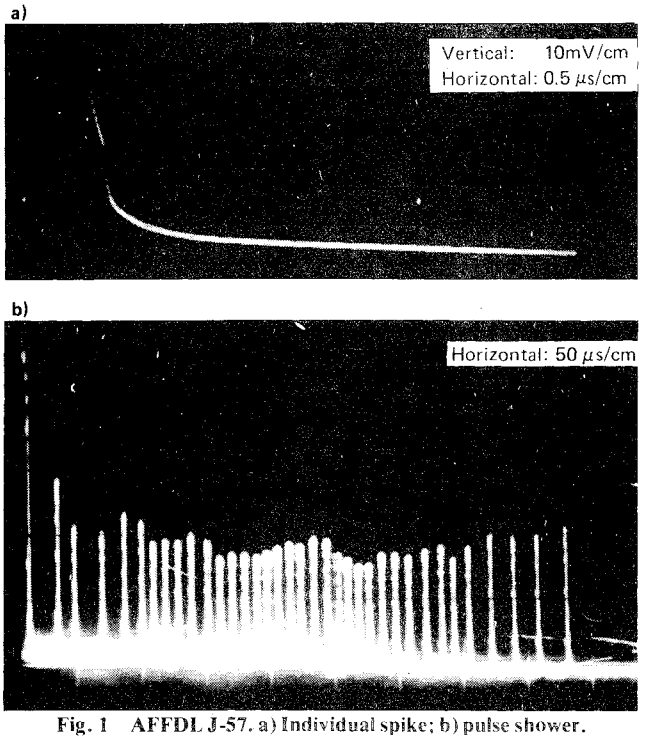

Fig. 1 AFFDL J-57. a) Individual spike; b) pulse shower.

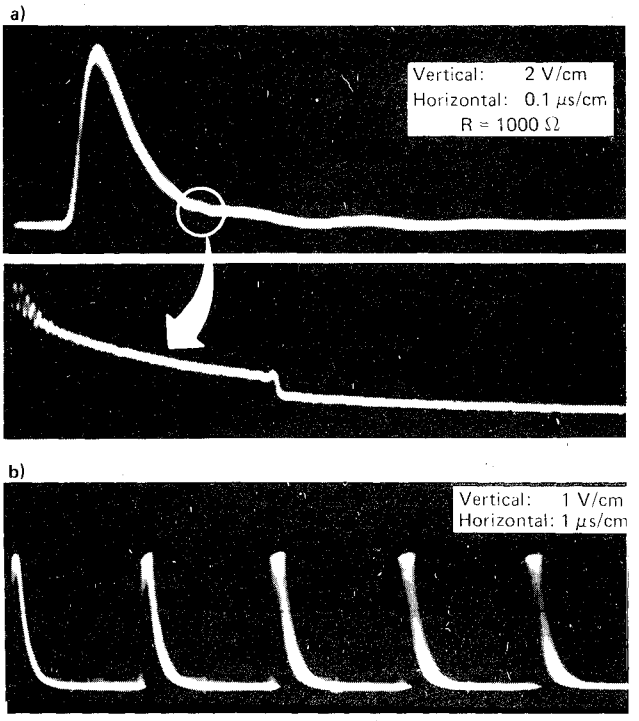

Fig. 2 Experiment. a) Single pulse with trailing-edge step; b) repetitive pulses.

entering the gas. A distinct feature of most pulses was slope change in the decay, signifying the onset of a different decay type.

In addition, showers of these pulses with time intervals ranging from 5 to 50 μs were observed (Fig. 1b) with the following features. 1) Pulse amplitude and rate were related; amplitudes were greatest for smallest pulse rates. 2) The first pulse was usually the largest; the magnitude then diminished for the first half of the shower and increased again for the second half. The pulse rate also varied, reaching a maximum in the middle. 3) Pulse showers sometimes changed into a noisy dc signal, and the shower was restarted within tens to hundreds of microseconds. This mode-change usually occurred when the pulse rate within the shower was quite high. 4) Pulses sometimes appeared superimposed on a more slowly varying, nearly dc voltage (i.e., on a nearly quasi-steady probe current, up to 100 μA in magnitude).

Simulated Spike Signal Experiment

Based on the data similarity, the probe spike phenomenon is interpreted to be a particular form of negative electrical discharge known as Trichel pulses. A negative corona discharge, however, requires the presence of a positive, high-potential source or "charged cloud." The evidence for the existence of such a charged cloud which moves with the exhaust gases is derived from a comparison of the spike data (showers) and the relationship between Trichel pulse height and repetition rate as a function of applied potential.

An experiment was conducted to illustrate the characteristics of Trichel pulses, including pulse shape, rise times, widths, pulses rates, and net charge per pulse. The electric field at the probe tip (cathode) is determined principally by the anode potential, by the probe tip radius of curvature, and by the probe-anode spacing. There is no electrical discharge at the anode. The anode serves only to apply an electric field at the probe tip, simulating the hypothesized charged cloud. One of the probes in this experiment was used by the AFFDL in their J-57 engine exhaust tests.

Upon application of a positive potential to the anode, there was no response until a certain onset level, when the discharge suddenly appeared. The discharge was then repetitive and steady, and each pulse had a distinctive step on the trailing edge (Fig. 2).

Increasing the positive inducing potential increased the pulse rate and changed the amplitude (Fig. 3). Increasing the anode potential caused the following. 1) The pulse amplitude increased rapidly, reached a maximum, and then decreased. 2) The pulse rate rapidly increased from 100 to 50,000 Hz and then increased more slowly to a maximum of $\sim 10^6$ Hz where the Trichel pulses gave way to a glow-mode type of discharge.

The high-temperature environment of the jet exhaust was qualitatively simulated by the flame of a propane torch placed at the probe tip. The effect of the flame reduced onset potentials and caused the pulsewidth to increase with a corresponding increase in the net charge per pulse. The maximum observed charge per pulse in these tests was $\sim$ 10 nC.

Engine spike data and Trichel pulse data are summarized in Table 1. The pulse shape from a J-57 engine is very similar to that of the Trichel pulse. The pulse polarities are both positive, and each has a similar rise time. The high-temperature Trichel pulsewidth has the same range as the probe data in the jet exhaust. The net charge for a single Trichel pulse and a spike are also in agreement. And finally, Trichel pulses and the engine spike signals both exhibit similar repetitive characteristics. Thus, spike signals from the jet-engine electrostatic probe are deduced to be Trichel pulses, a particular form of negative corona electrical discharge.

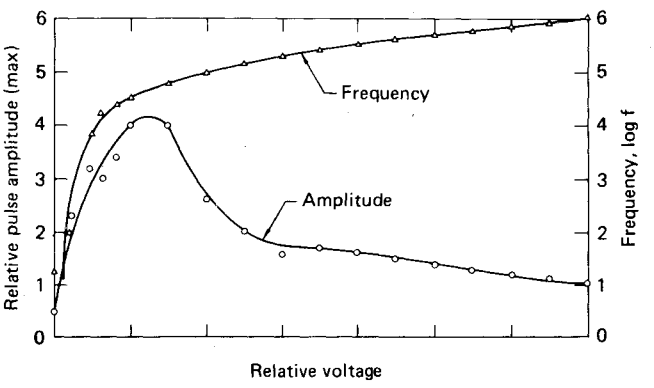

Fig. 3 Trichel pulse frequency and amplitude variation.

Table 1 Jet-engine spike and Trichel pulse comparison

Parameter	Jet engine exhaust	Trichel pulse
Polarity	Positive	Positive
Shape	Distinctive step on trailing edge	Distinctive step on trailing edge
Rise time	2 - 4 ns	< 10 ns
Net charge	0.1 - 10 nC	0.01 - 10 nC
Width	0.2 - 5 μs	0.01 - 5 μs
Repetition	Spike showers repetitive in nature - 10^5 - 10^6 Hz	Increasing frequency with increasing applied potential 100 - 10^6 Hz
	Increases then decreases in frequency	
Amplitude	Showers: first decreasing then increasing	Increasing then decreasing with applied potential

Evidence for Charged Clouds

In all our simulated experiments, Trichel pulses were obtained using a flat-plate anode. There is no obvious equivalent to such an anode in an engine exhaust/probe situation. Hence, a charged gas eddy or clouds associated with high electrical potentials must be postulated. Such clouds could be expected to move past the probe at the mean flow velocity. This charged cloud would not have to impact the probe, but should pass sufficiently close to induce probe-tip electric fields above the onset level.

The engine probe shower data support this postulate (Fig. 1b). These data show that the pulses at the start and finish of a shower have lower pulse rates and higher amplitudes than the pulses midway in the shower. These data are interpreted to indicate that the charged cloud is moving past the probe. As the cloud approaches and then recedes from the probe, the electric field at the probe tip increases, reaches a maximum, and then decreases. This phenomenon corresponds to Trichel pulse response as a function of applied voltage electric field; when the frequency exceeds 50 kHz, increasing the anode voltage increases the pulse rate and decreases the amplitude.

Charged-cloud properties can be estimated from the jet-engine spike probe data and our experimental results using the following assumptions. 1) The charged cloud moves with the jet exhaust gas exit velocity, ~ 305 m/s; 2) The cloud has a spherical shape. 3) The Trichel pulse onset potential for the blunt nose 0.563-cm AFFDL probe is 18 kV (where the value at room temperature was 26 kV and 12 kV in a propane flame). The cloud diameter is 15 cm based on the duration of a pulse shower, 500 μs (Fig. 1b), and the capacitance is 10 pF (for a sphere one body diameter above a ground plane). The net charge in the cloud is hence 180 nC with a resultant net charge density of 6×10^8 cm^{-3} and an electrostatic energy of 1.6 mJ. The cloud polarity is positive because an opposite sign would cause an anode corona at the probe tip whose properties would be far different from those of negative corona Trichel pulses. In particular, positive coronas are not known to display the well-defined repetition rates with frequencies up to several megahertz.

The sources of charged clouds have not been determined. Statistical evidence[3] indicates that they are related to certain engine failure modes and that their presence can be a warning of imminent engine failure. Three postulated mechanisms for producing charged clouds have been suggested,[1,2] particulate cloud, spray charging, and boundary-layer fluid accumulation.

Conclusions

The electrostatic probe spike signals observed in a jet-engine exhaust are deduced to be a particular form of negative electrical corona discharge known as Trichel pulses. Analyses of the spike shower data and known properties of Trichel pulses infer that the spike signals are induced by a positive, high-potential cloud which moves past the probe.

Acknowledgment

This work was supported by United States Air Force Flight Dynamics Laboratory, Contract No. F33615-74-C-3091.

References

[1]Shaeffer, J. F. and Peng, T. C., "High Potential Clouds in Jet Engine Exhausts," AIAA Paper 76-397, San Diego, Calif., 1976.

[2]Sajben, M., Peng, T. C., and Shaeffer, J. F., "Evaluation of Experiments using Electrostatic Probes to Detect Imminent Failure of Jet-Engine Gas-Path Components," Air Force Flight Dynamics Lab, Wright Patterson, AFB, Ohio, AFFDL TR-75-74, July 1975.

[3]Couch, R. P. and Rossbach, D. R., "Sensing Jet Engine Performance and Incipient Failure with Electrostatic Probes," Air Force Dynamics Lab, Wright Patterson, AFB, Ohio, AFFDL TR-71-173, Dec. 1972.

Velocity-Temperature Relations in Turbulent Boundary Layers with Nonunity Prandtl Numbers

D. L. Whitfield* and M. D. High†
ARO, Inc., Arnold Air Force Station, Tenn.

Nomenclature

A $= (\gamma - 1) M_\infty^2$
f = function defined by Eq. (8)
H = specific total enthalpy
$\bar{H}_\infty$ $= H_\infty / h_\infty = 1 + A/2$
h = specific enthalpy
$\bar{h}$ $= h/h_\infty$
$\bar{h}_0$ = zeroth-order $\bar{h}$
$\bar{h}_1$ = first-order $\bar{h}$
k = molecular thermal conductivity
k_t = eddy thermal conductivity
M = Mach number
m $= u = \eta^{1/m}$, used herein as $m = 7$
Pr_m = mixed Prandtl number, $c_p(\mu + \mu_t)/(k + k_t)$
r = recovery factor, $r = (T_{aw} - T_\infty)/(T_{0,\infty} - T_\infty)$
T = mean static temperature
T_0 = local total temperature
$\bar{T}$ $= (T_0 - T_w)/(T_{0,\infty} - T_w)$
u = mean flow velocity
$\bar{u}$ $= u/u_\infty$
u_τ $= u/(\tau_w/\rho_w)^{1/2}$
Y = distance normal to surface
α $= (5/2)m$
γ = ratio of specific heats
Δ = defined by Eq. (10) for constant temperature wall and by Eq. (13) for an adiabatic wall
δ = boundary-layer thickness
ϵ $= 1 - Pr_m$
η $= Y/\delta$
μ = molecular viscosity
μ_t = eddy viscosity

Presented as Paper 76-411 at the AIAA 9th Fluid and Plasma Dynamics Conference, San Diego, Calif., July 14-16, 1976; submitted July 23, 1976; revision received Nov. 24, 1976.

Index category: Boundary Layers and Convective Heat Transfer – Turbulent.

*Supervisor, Analysis Section, 16T/S Projects Branch, Propulsion Wind-Tunnel Facility. Member AIAA.

†Assistant Branch Manager, 16T/S Projects Branch, Propulsion Wind-Tunnel Facility. Associate Fellow AIAA.